International Journal of Natural and Engineering Sciences
E-ISSN: 2146-0086 18(1): 32-44, 2024
Research Article

A comparative study on the natural ventilation performance in buildings with different roof shapes

Rupam Deka[1,*], Kalyan Kumar Das [2], Dipankar Das [1], Madhurjya Saikia [1]
Pranjal Sarmah[1]

[1]*Department of Mechanical Engineering, Dibrugarh University, Dibrugarh, India*
[2]*Department of Mechanical Engineering, Assam Engineering College, Guwahati, India*

*Corresponding author: rupamdeka@dibru.ac.in

(Received: January 4, 2024 / Accepted: March 6, 2024)

Abstract

The extensive use of mechanical ventilation systems is severely impacting the environment as these systems are one of the major sources of greenhouse gas emissions. Natural ventilation can effectively replace mechanical ventilation systems if the performance of the former is enhanced. The performance of a natural ventilation system depends on many factors such as the geometry of the building, opening size, shape, and positions. The studies related to quantitative analysis of natural ventilation performance in buildings are limited. Even though some of the studies have investigated the performance of natural ventilation in flat-roof buildings, however, completely ignore gable roof buildings. Considering the widespread usage of gable roof structures it is highly significant to investigate the natural ventilation performance in gable roof buildings. Thus, in this work, the quantitative assessment of natural ventilation performance in gable roof buildings has been investigated and compared with the flat roof buildings using computational fluid dynamics (CFD). Six different configurations based on the relative locations of the windward and leeward openings were considered for both roof shapes. Numerical simulations were carried out using ANSYS-FLUENT software to investigate the ventilation performance for each of the configurations. The three parameters selected for evaluating the natural ventilation performance are normalized average velocity magnitude (V^*), velocity homogeneity index, H, and normalized volumetric flow, Q^*. The results showed that the flat roof configurations have higher values of V^* and H which infers that flat roof configurations have better natural ventilation performance than gable roof configurations. Moreover, among the six configurations tested the configuration with windward opening below the mid-height and the leeward opening above the mid-height of the building wall has the best natural ventilation performance. The configuration with the windward opening at the mid-height and leeward opening below the mid-height of the building wall has the highest volume flow rate.

Keywords: global warming, natural ventilation, numerical simulation, indoor air quality, thermal comfort.

Introduction

Ventilation is an integral part of the building construction. In buildings, ventilation is accomplished primarily by two modes natural ventilation and mechanical ventilation. Natural ventilation is becoming a preferred choice due to its various advantages over mechanical ventilation. To operate mechanical ventilation systems energy is required however natural ventilation consumes no energy. Moreover, mechanical ventilation systems emit greenhouse gases which are a major cause of concern as the threat of global warming looms on the planet Earth. Natural ventilation is of two types- wind-driven which is basically due to pressure gradient and buoyancy-driven due to temperature gradient. It facilitates the exchange of internal and external air in buildings. As the heat is carried away from inside the building it helps in maintaining a thermally comfortable indoor environment. Furthermore, due to the mixing of internal and external air, the concentration level of pollutants inside the building lowers which improves the indoor air quality. Natural ventilation also helps in expelling harmful contaminants inside the building.

Buildings are one of the important elements of the urban infrastructure. As the wind interacts with buildings the wind environment around it is significantly affected which results in a change in the pressure distribution influencing the natural ventilation. The flow field produced by the wind is significantly affected by the geometry of the building [1-4]. Buildings have different geometry due to the shape of the roofs. Various

building geometries are- flat roofs, gable or pitched roofs, arched or curved roofs, and sawtooth roofs. Among these flat and gable roof structures are most common. The roof shape has a remarkable impact on the wind-induced flow field eventually affecting the natural ventilation. Various studies have been conducted in the past to investigate natural ventilation in flat and gable roof buildings. Three methods- full-scale measurements, wind tunnel experiments, and numerical simulations are primarily carried out in natural ventilation investigations. Katayama et al. [5] employed both full-scale measurements and wind tunnel experiments however; Iino et al. [6] used wind tunnel experiments and numerical simulations to analyze the cross-ventilation characteristics in flat roof buildings. Ohba et al. [7] and True [8] also investigated cross-ventilation in flat-roof buildings. Karava et al. [9] carried out a series of experiments to study cross-ventilation. The results of numerical simulations of cross-ventilation problems are affected by different parameters. Ramponi and Blocken [10] attempted to analyze the impact of these parameters. The influence of building length on cross-ventilation was investigated by Chu and Chiang [11]. Cross-ventilation through vertical openings was studied by Manolesos et al., [12]. A systematic study on the comparison of single-sided and cross-ventilation was undertaken by Zhang et al., [13]. Furthermore, Moey et al., [14] attempted to study the effect of non-aligned openings on cross-ventilation. Gable or pitched roof buildings are most commonly used in schools, hospitals, and residential and commercial buildings. Although many researchers considered flat roof buildings in the investigation of cross-ventilation however, some researchers also worked on gable roof buildings [15, 16]. The effect of internal pressure on the cross-ventilation was investigated by Karava et al. [17]. Most of the studies considered ventilation or airing through windows however, cross ventilation through doors in a gable roof building was studied by Kobayashi et al., [18]. A series of wind tunnel experiments were performed by Yi et al., [19] to study the indoor airflow pattern in a naturally ventilated dairy burn. The wind-induced flow field around an isolated gable-roof building with and without openings was studied by Xing et al. [20]. Hayati et al., [21] also performed both wind tunnel experiments and numerical simulations to investigate airing through doors. Apart from the flat and gable roof structures, the investigation of natural ventilation through buildings with arched roofs [22] and sawtooth roofs [23, 24] has also been carried out previously.

Although various studies have been carried out in the past to investigate the cross-ventilation flow only a few studies have attempted to investigate the natural ventilation performance quantitatively. Díaz-Calderón et al.[25] evaluated the performance of natural ventilation using three parameters namely, normalized average velocity magnitude (V^*), velocity homogeneity index (H), and normalized volumetric flow (Q^*). However, their study mainly focussed on flat-roof buildings. Since gable roof buildings are also quite prevalent in both urban and rural areas hence, the evaluation of ventilation performance in gable roof buildings is highly crucial. Therefore, in the present study, the ventilation performance in gable roof buildings is evaluated quantitatively and compared with flat roof buildings. The study primarily aims to identify a suitable configuration with optimum ventilation performance.

Methodology-Numerical simulation

The detailed methodology adopted to perform the numerical simulations has been discussed in this section.

Building models and configurations

In the present study, the natural ventilation performance of flat and gable roof buildings is analyzed numerically. The gable roof building model considered herein has a width (w) of 6 m, length (l) of 12 m, and eave height (h) of 6 m respectively, and a roof pitch of 5:10 (Figure 1(a)). Furthermore, for the flat roof building model, the width (w) and length (l) are kept the same i.e. 6 m and 12 m respectively. However, the height (h) of the flat roof model is set as 6.75 m (Figure 1(b)) to ensure the same volume for both flat and gable roof buildings.

The analysis is performed for six different configurations each for flat and gable roof buildings. These configurations are chosen such that the openings are located in opposite facades and are non-aligned. Further, the opening size for all the configurations is identical i.e. 6 m × 1.2 m ($w \times h$). The vertical positions of the openings on the windward and leeward facades of these six configurations namely A, B, C, D, E, and F are shown in Figure 2.

Computational domain and grid

The computational domain created for performing the numerical simulations has a downstream length of 15h and lateral and vertical lengths are set as 5h each where h is the height of the building model (Figure 3(a)). These dimensions are specified based on the best practice guidelines suggested by Franke et al., [26] and Tominaga et al., [27]. Furthermore, the upstream length has been kept at 3h as suggested by Blocken et al., [28] (Figure 3(a)).

Hybrid mesh is developed with tetrahedron and hexahedral elements near and away from the building model and prism layers are generated near the solid boundary (Figure 3(b)). The mesh density was made finer near the building model. Numerical simulations are performed by employing similar grids for both the flat and gable roof building models.

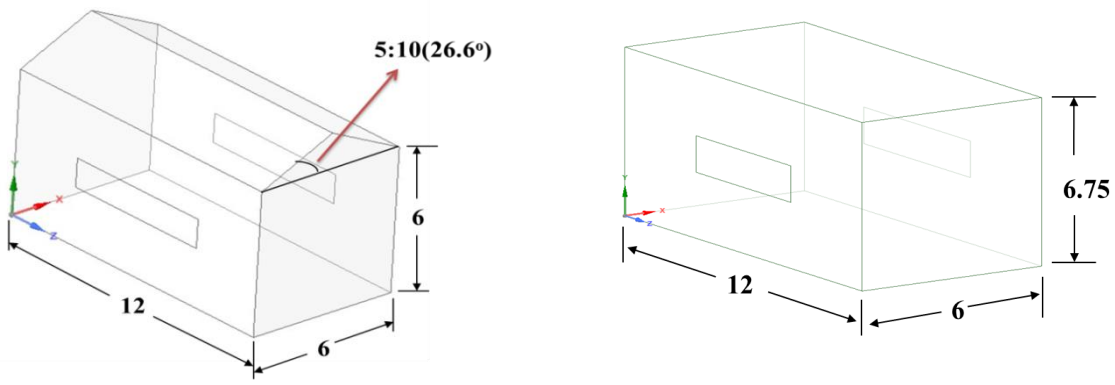

(All Dimensions are in m)

(a) ***(b)***

Figure 1. *Schematic view of the building model (a) Gable roof (b) Flat roof*

Boundary conditions and solver settings

For the simulations, the inlet velocity profile employed was based on the logarithmic law as given in Equation 1

$$U(y) = \frac{u^*_{ABL}}{\kappa} \ln\left(\frac{y + y_o}{y_o}\right) \qquad \textbf{Equation 1}$$

Where, the friction velocity u^*_{ABL} is 0.347 m/s, which is determined from the reference velocity (U_{ref} =10 m/s) at a height (y_{ref}=h=6 m) [29], the aerodynamic roughness length (y_o=0.0001 m), and y is the height coordinate and κ is Von Karman constant (κ=0.4).

The profile of the turbulent kinetic energy at the inlet is given by

$$k(y) = a\left(I_u(y).u(y)\right)^2 \qquad \textbf{Equation 2}$$

In Equation 2, as recommended by Tominaga et al., [27] the value of 'a' was selected as 1 (a=1) and the profile of streamwise turbulent intensity is chosen according to the equation (3) as obtained by [30].

$$I_u(y) = \frac{1}{\ln\left(\frac{y}{y_o}\right)} \qquad \textbf{Equation 3}$$

At the inlet, the profile used for the turbulent dissipation rate (ε) and the specific dissipation rate (ω) are defined in Equations 4 and 5 respectively

$$\varepsilon(y) = \frac{u_{ABL}^{*3}}{\kappa(y + y_o)} \qquad \textbf{Equation 4}$$

$$\omega(y) = \frac{\varepsilon(y)}{C_\mu k(y)} \qquad \textbf{Equation 5}$$

Where Cμ is an empirical constant taken as 0.09.

The roughness constant and roughness height for the building surfaces are taken as 0.5 and 0. Symmetry boundary conditions were imposed on the sides and top of the domain with zero normal velocity and zero gradients for all variables. The outlet of the domain was imposed with zero static pressure.

For the ground surface, the roughness constant C_s was assumed as 1, and the sand grain roughness height k_s could be determined using Equation 6 according to their relationship with aerodynamic roughness length, y_o

$$k_s = \frac{9.793 y_o}{C_s} \qquad \textbf{Equation 6}$$

To investigate the wind-driven natural ventilation in low-rise buildings the steady state flow simulations are performed in commercial CFD software package ANSYS-FLUENT version 19. The 3D steady RANS equations are solved using the k-ω SST turbulence model. For pressure-velocity coupling, the SIMPLE algorithm was employed. The pressure interpolation is of the second order, and all other transport equations are discretized by a second-order upwind scheme. Convergence is assumed to be obtained when all the scaled residuals leveled off reached a minimum of 10^{-5} for Continuity, x, y, z momentum and k, and 10^{-4} for ω. Since oscillatory convergence was observed for the simulations hence, initial simulations were carried out for 5000 iterations and the results were sampled and averaged over the last 500 iterations as also done by [10]. Additionally, the stream-wise wind speed (U) was monitored at three different points in the domain- at the center and upstream and downstream location of the building.

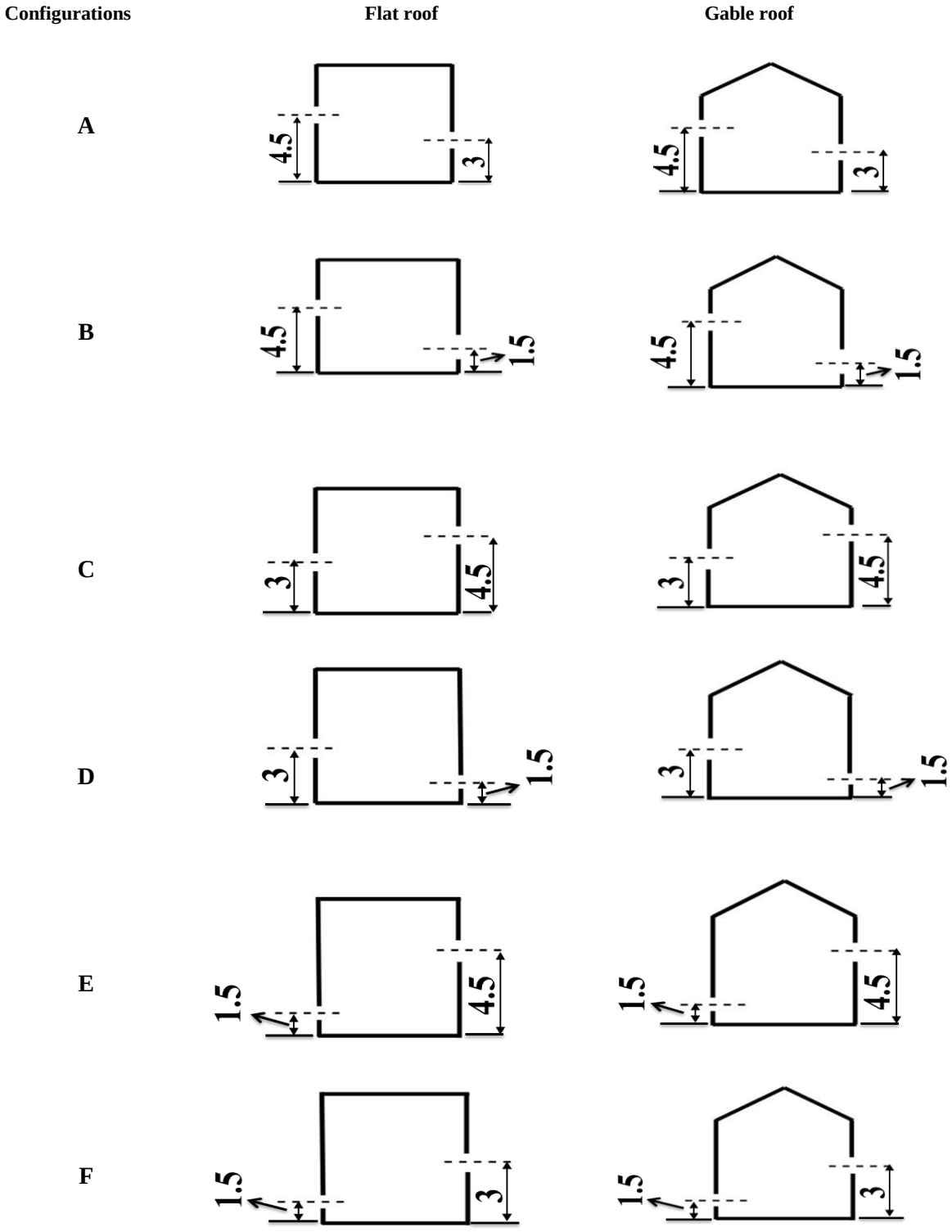

Figure 2. *Different building configurations with pair of non-aligned openings*

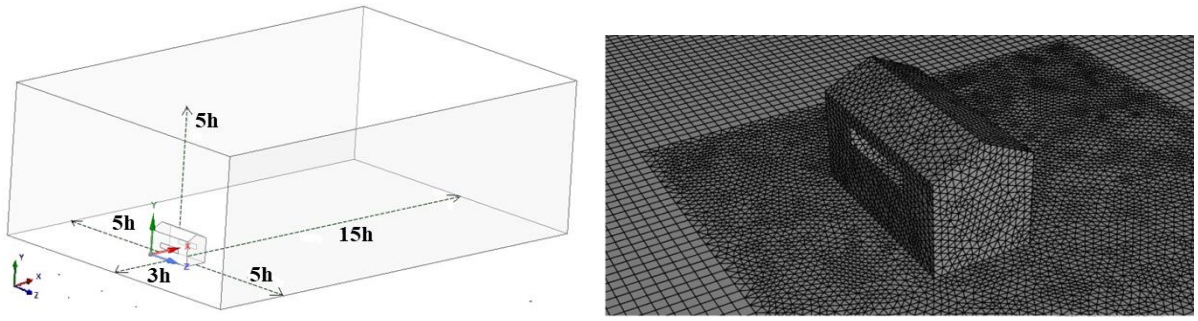

(a) **(b)**

Figure 3. *Computational domain (a) perspective view with dimensions (b) with generated grid*

Validation

Validation is a crucial step in CFD simulations. The experimental work done by Karava et al. [31] to study the cross-ventilation in a building using the PIV technique is considered as the benchmark for the validation of current numerical simulations. Additionally, Ramponi and Blocken [10] also attempted to reproduce the experimental results of [31] numerically. Hence, in the present work, the results obtained from the CFD simulations are compared with both the experimental results of [31] and the results obtained from the numerical simulations carried out by [10]. The configuration considered for this purpose comprises two openings placed at the mid-height of windward and leeward facades. The variation of normalized streamwise wind speed (U/U_{ref}) along the horizontal line passing through the center of the windward and the leeward opening is compared in Figure 4. The results obtained from the present CFD simulations are found to be in good agreement with [10]. However, minor deviations can be observed between the experimental and the numerical results. The reasons for the deviations can be attributed to the limitations of PIV measurements.

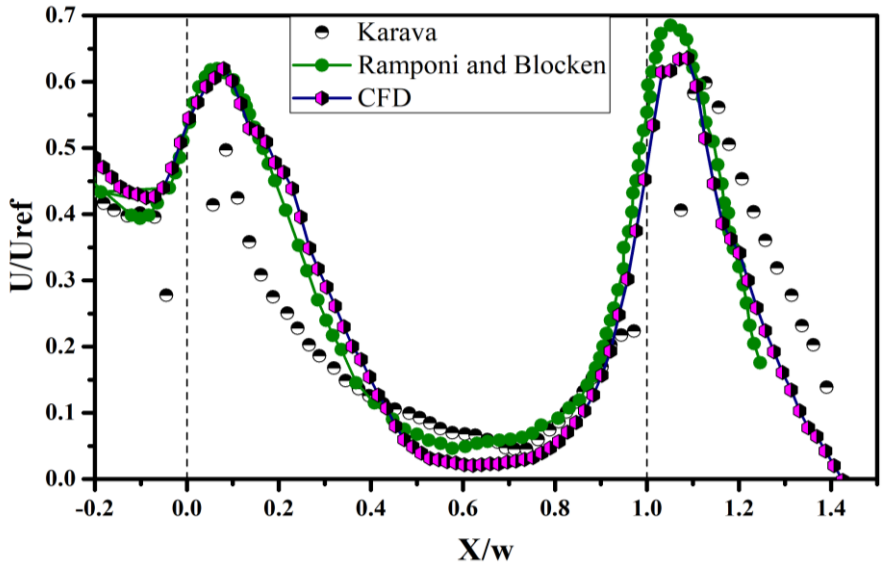

Figure 4. *Comparison of normalized streamwise wind speed (U/U_{ref}) along the horizontal line passing through the center of the windward and leeward opening obtained from PIV measurements and numerical simulations*

Results and Discussion

To assess the natural ventilation performance in a living zone, Daiz et al. [25] proposed three parameters namely the normalized average velocity magnitude (V^*), velocity homogeneity index (H), and normalized volumetric flow (Q^*). The entire inner air volume of the building is considered to be the living zone in this study. Here, the V^* and H are related to indoor air distribution. The higher values of V^* and H indicate better indoor air quality. Further, Q^* is associated with thermal comfort as it is a measure of heat-carrying capacity from the living zone. Therefore, to investigate the natural ventilation performance in flat and gable roof structures, the aforementioned parameters (V^*, H, and Q^*) are evaluated for each of the six configurations in the living zone using numerical simulations.

The normalized average velocity magnitude can be defined as follows-

$$V^* = \frac{V_{avg}}{U_{ref}} \qquad \textbf{Equation 7}$$

Where V_{avg} is the average velocity magnitude in the living zone and U_{ref} is the reference velocity at the eave height of the gable roof building (h=6 m).

The parameter velocity homogeneity index, H is estimated as given by Cruz-Salas et al. [32]

$$H = 1 - \frac{\sigma_V}{V_{avg}} \qquad \textbf{Equation 8}$$

where σ_V is the standard deviation of velocity magnitude in the living zone.

The normalized volumetric flow, Q^* is mathematically expressed as

$$Q^* = \frac{Q}{Q_{ref}} \qquad \textbf{Equation 9}$$

where Q is the volume flow rate calculated using the CFD technique and $Q_{ref} = A_o\, U_{ref}$; A_o is the opening area.

Comparison of normalized average velocity magnitude (V*) in flat and gable roof configurations

It is worth mentioning here that, the higher value of V^* signifies a better mixing of air in the living zone. Hence, with the higher magnitude of V^* the indoor air quality improves significantly which eventually improves the natural ventilation performance. Therefore, simulations were performed to evaluate the V^* for both gable and flat roof buildings with all six different opening configurations and the results are presented in Figure 5. It is observed that for both flat and gable roofs the highest value of V^* is obtained for configuration E, and the least for configuration D. The difference between the highest and the least value of V^* among the six configurations considered is noted to be 58.98% in flat roof buildings and 33.40% in gable roof buildings. Another important observation is that the configurations having windward openings below the mid-height (i.e. configuration E and F) show higher values of V^*. Further, it is to be noted that, in general V^* is higher in the flat roof configurations as compared to gable roof, except for configuration D where the V^* is almost equal. For configuration E, the V^* is found to be 17.69 % higher for flat roofs as compared to gable roof buildings.

Comparison of velocity homogeneity index (H) in flat and gable roof configurations

From the same set of simulations as mentioned in the previous section, the velocity homogeneity index (*H*) is evaluated for all the configurations. Figure 6 presents the comparison of the velocity homogeneity index (*H*) for flat and gable roof buildings with various opening configurations. Here, the value of *H* is noted to be highest for configuration E and lowest for configuration D irrespective of the shape of the building. There is a 155% increment of *H* is observed between the highest and the lowest value of *H* in flat roof configurations as against a 145% increment in gable roof configurations. Similar to *V**, irrespective of the shape of the building, the value of H is found to be higher for configurations (i.e. configuration E and F) with windward openings below the mid-height. Furthermore, for similar configurations, the magnitude of *H* is higher in flat roofs as compared to gable roof buildings for all the configurations. For configuration E (with the highest *H*), the value of *H* is 13.24% higher for the flat-roof building. Another important observation is that although the difference in magnitude of *V** between the flat and gable roof buildings for configuration D is negligible, however, the flat roof has an 8.94% higher value of *H* than the gable roof structure. It is worth noting here that the higher value of *H* signifies better natural ventilation performance.

Comparison of normalized volumetric flow (Q*) in flat and gable roof buildings

The investigation continued to evaluate the normalized volumetric flow (Q*), which is an important parameter to measure the heat-carrying capacity. The higher value of Q* indicates that it carries away more heat from the living zone leading to the cooling of the space which is beneficial in the summer season. However, it is unwanted during the winter season. Hence, Q* is strongly related to the thermal comfort of the living zone rather than the internal air quality. Figure 7 shows the comparison of the normalized volumetric flow (Q*) for flat and gable roof buildings with six different non-aligned opening configurations. For both flat and gable roof buildings, the normalized volume flow rate is found to be the maximum for configuration D, where the windward opening is at the mid-height and the leeward opening below the mid-height. Q* is the minimum for configuration E having a windward opening below the mid-height and a leeward opening above the mid-height. The difference between the maximum and minimum value of Q* among the six configurations is found to be 35.08% and 38.94% for flat and gable roof configurations respectively. Furthermore, for configurations A, B, and C; Q* is higher in flat roofs. However, for configuration D, Q* is higher by 2.89 % for gable roof building. For the rest of the configurations (E and F), Q* is noted to be equivalent. Overall it can be said that for identical configurations the difference in Q* between the flat and gable roof buildings is less significant.

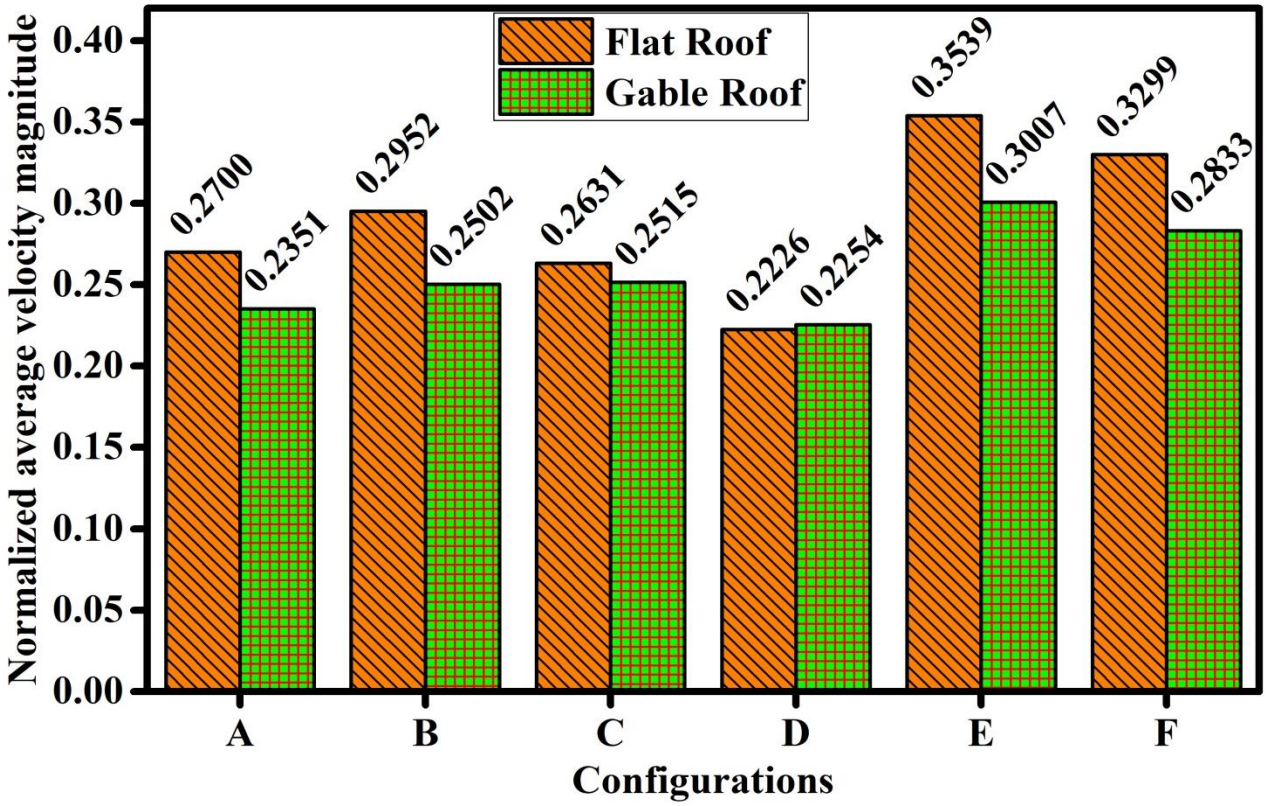

Figure 5. *Comparison of normalized average velocity magnitude (V*) in flat and gable roof buildings for six different configurations*

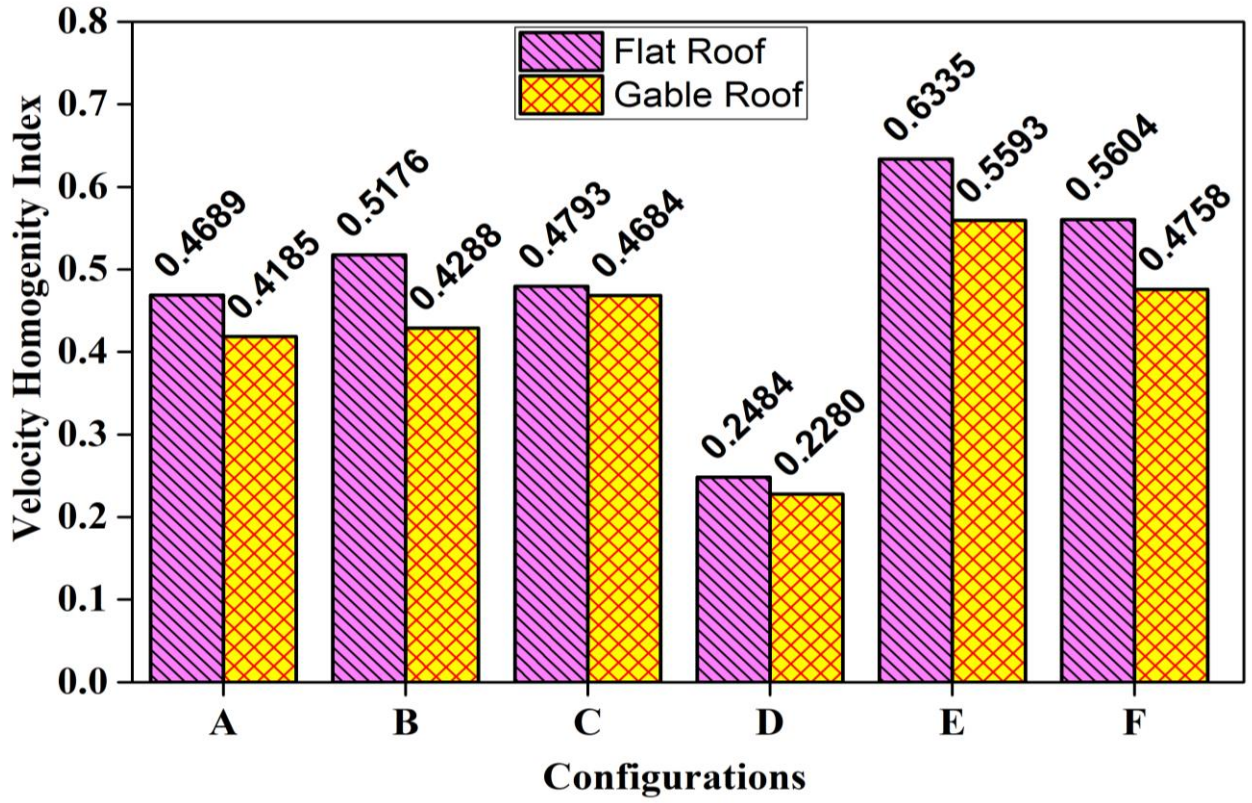

Figure 6. *Comparison of velocity homogeneity index(H) in flat and gable roof buildings for six different configurations*

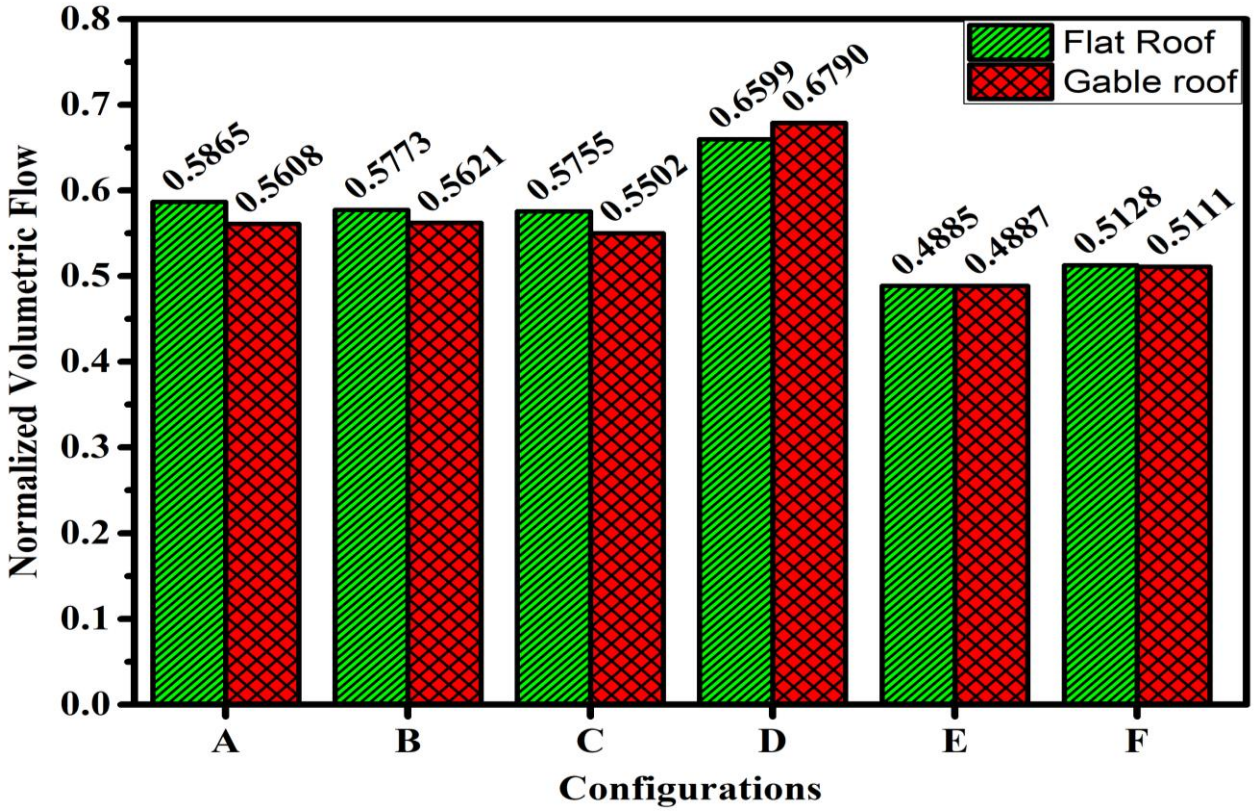

Figure 7. *Comparison of normalized volumetric flow (Q*) in flat and gable roof buildings for six different configurations*

Conclusion

In this work, a comparative study on the ventilation performance in flat and gable roof buildings has been carried out. Six different opening configurations are considered for the present study. Numerical simulations are carried out using ANSYS-FLUENT commercial CFD software. The parameters considered for assessment of the natural ventilation performance are normalized average velocity magnitude (V^*), velocity homogeneity Index (H), and normalized volumetric flow (Q^*). Among the six configurations analyzed for both flat and gable roof buildings, the configurations having windward openings below the mid-height (i.e. configuration E and F) show higher values of V^* and H compared to other configurations. Furthermore, irrespective of the roof shape, the peak values of V^* and H are obtained for configuration E; where the windward opening is located below the mid-height and the leeward opening is located above the mid-height. As the higher value of V^* and H signifies better air quality in the living zone, hence it can be concluded that configuration E would provide the best natural ventilation performance in both flat and gable roof buildings. Moreover, for both the roof shapes the least value of V^* and H are noted in the case of configuration D resulting in poor natural ventilation performance. In addition, it is found that irrespective of the location of the openings, flat roof configurations have higher values of V^* and H compared to the gable roof building. Therefore, it can be concluded that the flat roof configurations have better natural ventilation performance than gable roof configurations. Furthermore, the analysis of Q^*, reveals that irrespective of the roof shape, configuration D has the highest and configuration E the least volume flow rate. Hence it can be concluded that configuration D has the enhanced capacity to carry away the heat from the living zone resulting in the cooling of the inner space. Thus configuration D is suitable for the summer season. In contrast to that configuration E, is preferred in the winter season as it has a lower heat-carrying capacity.

References

[1] Sousa, J. M. M., and Pereira, J. C. F. (2004). DPIV study of the effect of a gable roof on the flow structure around a surface-mounted cubic obstacle. Experiments in Fluids. 37(3): 409–418. DOI: https://doi.org/10.1007/s00348-004-0830-2

[2] Irwin, P. A. (2008). Bluff body aerodynamics in wind engineering. Journal of Wind Engineering and Industrial Aerodynamics. 96(6–7): 701–712. DOI : https://doi.org/10.1016/j.jweia.2007.06.008

[3] Mooneghi, M. A., Irwin, P., and Chowdhury, A.G. (2016). Partial turbulence simulation method for predicting peak wind loads on small structures and building appurtenances. Journal of Wind Engineering and Industrial Aerodynamics. 157:47–62. DOI: https://doi.org/10.1016/j.jweia.2016.08.003

[4] Xing, F., Mohotti, D., and Chauhan, K. (2018). Study on localised wind pressure development in gable roof buildings having different roof pitches with experiments, RANS and LES simulation models. Building and Environment. 143 : 240–257. DOI: https://doi.org/10.1016/j.buildenv.2018.07.026

[5] Katayama, T., Tsutsumi, J., and Ishii, A. (1992). Full-scale measurements and wind tunnel tests on cross-ventilation. Journal of Wind Engineering and Industrial Aerodynamics. 41–44:2553–2562. DOI: https://doi.org/10.1016/0167-6105(92)90047-E

[6] Iino, Y., Kurabuchi T., Kobayashi N., and Arashiguchi, A. (1998). Study on airflow characteristics in and around building induced by cross-ventilation using wind tunnel experiments and CFD simulation. Sixth International Conference on Air Distribution in Rooms. 2: 307–314.

[7] Ohba, M., Irie, K. and Kurabuchi T. (2001). Study on airflow characteristics inside and outside a cross-ventilation model, and ventilation flow rates using wind tunnel experiments. Journal of Wind Engineering and Industrial Aerodynamics. 89:1513-1524. DOI: https://doi.org/10.1016/S0167-6105(01)00130-1

[8] True, J. P. J. (2003). Openings in Wind Driven Natural Ventilation. Ph.D. Thesis. Department of Building Technology and Structural Engineering, Aalborg University, Denmark.

[9] Karava, P., Stathopoulos, T., and Athienitis, A. K. (2005). Wind driven flow through building openings. Proceedings of International Conference on Passive and Low Energy Cooling for the Built Environment. 427–432.

[10] Ramponi, R., and Blocken, B. (2012). CFD simulation of cross-ventilation flow for different isolated building configurations: Validation with wind tunnel measurements and analysis of physical and numerical diffusion effects. Journal of Wind Engineering and Industrial Aerodynamics. 104–106: 408–418. DOI: https://doi.org/ 10.1016/j.jweia.2012.02.005

[11] Chu, C. R., and Chiang, B. F. (2014). Wind-driven cross ventilation in long buildings. Building and Environment. 80: 150–158. DOI: https://doi.org/ 10.1016/j.buildenv.2014.05.017

[12] Manolesos, M., Gao, Z., and Bouris, D. (2018). Experimental investigation of the atmospheric boundary layer flow past a building model with openings. Building and Environment. 141: 166–181. DOI: https://doi.org/ 10.1016/j.buildenv.2018.05.049

[13] Zhang, X., Weerasuriya, A. U., and Tse, K. T. (2020). CFD Simulation of Natural Ventilation of a Generic Building in Various Incident Wind Directions : Comparison of Turbulence Modelling, Evaluation Methods, and Ventilation Mechanisms". Energy and Buildings. 229:110516. DOI: https://doi.org/ 10.1016/j.enbuild.2020.110516

[14] Moey, L. K., Chan, K. L., Tai, V. C., Go, T. F., and Chong, P. L. (2021). Investigation on the effect of opening position across an isolated building for wind-driven cross ventilation. Journal of Mechanical Engineering and Sciences. 15(2): 8141–8152. DOI: https://doi.org/ 10.15282/jmes.15.2.2021.14.0639

[15] Vickery, B. J., Baddour, R.E., and Karakatsanis, C. A. (1983). Study of the external wind pressure distributions and induced internal ventilation flow in low-rise industrial and domestic structures. Technical Report No. BLWT-SS2-1983, United States.

[16] Vickery, B. J. and Karakatsanis, C. (1987). External wind pressure distributions and induced internal ventilation flow in low-rise industrial and domestic structures. ASHRAE Transactions, vol. 93(2), pp. 2198- 2213.

[17] Karava, P., Stathopoulos, T. and Athienitis, A. K. (2006). Impact of Internal Pressure Coefficients on Wind-Driven Ventilation Analysis. International Journal of Ventilation. 5(1):53-66. http://dx.doi.org/10.1080/14733315.2006.11683724

[18] Kobayashi, T., Sandberg, M., Kotani, H., and Claesson, L. (2010). Experimental investigation and CFD analysis of cross-ventilated flow through single room detached house model. Building and Environment. 45(12):2723–2734. http://dx.doi.org/10.1016/j.buildenv.2010.06.001

[19] Yi, Q., König, M., Janke, D., Hempel, S., Zhang, G., Amon, B., and Amon, T. (2018). Wind tunnel investigations of sidewall opening effects on indoor airflows of a cross-ventilated dairy building. Energy and Buildings. 175:163–172. http://dx.doi.org/ 10.1016/j.enbuild.2018.07.026

[20] Xing, F., Mohotti, D., and Chauhan, K. (2018). Experimental and numerical study on mean pressure distributions around an isolated gable roof building with and without openings. Building and Environment.132: 30–44. https://doi.org/10.1016/j.buildenv.2018.01.027

[21] Hayati, A., Mattsson, M., and Sandberg, M. (2018). A wind tunnel study of wind-driven airing through open doors. International Journal of Ventilation. 18(2):113–135. https://doi.org/10.1080/14733315.2018.1435027

[22] Esfeh, M. K., Sohankar, A., Shahsavari, A. R., Rastan, M. R., Ghodrat, M., and Nili, M. (2021). Experimental and numerical evaluation of wind-driven natural ventilation of a curved roof for various wind angles. Building and Environment. 205 (August): 108275. https://doi.org/10.1016/j.buildenv.2021.108275

[23] Perén, J. I., van Hooff, T., Leite, B. C. C., and Blocken, B. (2015). CFD analysis of cross-ventilation of a generic isolated building with asymmetric opening positions: Impact of roof angle and opening location. Building and Environment. 85: 263–276. http://dx.doi.org/10.1016/j.buildenv.2014.12.007

[24] Perén, J. I., van Hooff, T., Leite, B. C. C., and Blocken, B. (2016). CFD simulation of wind-driven upward cross ventilation and its enhancement in long buildings: Impact of single-span versus double-span leeward sawtooth roof and opening ratio. Building and Environment. 96:142–156. http://dx.doi.org/10.1016/j.buildenv.2015.11.021

[25] Díaz-Calderón, S. F., Castillo, J. A., and Huelsz, G. (2023). Evaluation of different window heights and facade porosities in naturally cross-ventilated buildings: CFD validation. Journal of Wind Engineering and Industrial Aerodynamics. 232: 105263. https://doi.org/10.1016/j.jweia.2022.105263

[26] Franke, J., Hellsten, A., Schlünzen, H., and Carissimo, B. (2007). Best Practice Guideline for the CFD Simulation of Flows in the Urban Environment. Brussels: COST Office.

[27] Tominaga, Y., Mochida, A., Yoshie, R., Kataoka, H., Nozu, T., Yoshikawa, M., and Shirasawa, T. (2008). AIJ guidelines for practical applications of CFD to pedestrian wind environment around buildings. Journal of Wind Engineering and Industrial Aerodynamics.96 (10–11):1749–1761. https://doi.org/10.1016/j.jweia.2008.02.058

[28] Blocken, B., Stathopoulos, T., and Carmeliet, J. (2007). CFD simulation of the atmospheric boundary layer: wall function problems. Atmospheric Environment. 41(2):238–252. https://doi.org/ 10.1016/j.atmosenv.2006.08.019

[29] Hargreaves D.M. and Wright N.G. (2006). The use of commercial CFD software to model the atmospheric boundary layer. The Fourth International Symposium on Computational Wind Engineering (CWE 2006), Yokohama.

[30] Karava, P. (2008). Airflow Prediction in buildings for Natural Ventilation Design: wind tunnel measurements and simulation. Ph. D. Dissertation, Department of Building, Civil and Environmental Engineering, Concordia University, Montreal, Canada.

[31] Karava, P., Stathopoulos, T., and Athienitis, A. K. (2011). Airflow assessment in cross-ventilated buildings with operable façade elements. Building and Environment. 46(1):266–279. https://doi.org/10.1016/j.buildenv.2010.07.022

[32] Cruz-Salas, M., Castillo, J., Huelsz, G. (2018). Effect of wind exchanger duct cross-section area and geometry on the room airflow distribution. Journal of Wind Engineering and Industrial Aerodynamics. 179: 514–523. https://doi.org/10.1016/j.jweia.2018.06.022